A Late Glacial-early Holocene multiproxy record from the eastern Fram Strait, Polar North Atlantic

S. Aagaard-Sørensen[a*], K. Husum[a,b], K. Werner[c,d], R.F. Spielhagen[d,e], M. Hald[a], T.M. Marchitto[f]

[a] Department of Geology, University of Tromsø, 9037 Tromsø, Norway;

[b] Norwegian Polar Institute, Framsenteret, 9296 Tromsø, Norway

[c] Byrd Polar Research Center, Ohio State University, 1090 Carmack Road, 43210 Columbus OH, USA

[d] GEOMAR Helmholtz Centre for Ocean Research Kiel, Wischhofstraße 1-3, D-24148 Kiel, Germany

[e] Academy of Sciences, Humanities, and Literature, 55131 Mainz, Germany

[f] Department of Geological Sciences and Institute of Arctic and Alpine Research, University of Colorado, Campus Box 450, Boulder, Colorado 80309, USA

[*] Corresponding author. Tel.: +47 776 46374; Fax.: +47 77 64 56 00; E-mail address: Steffen.Sorensen@uit.no

Abstract

The paleoceanographic development of the eastern Fram Strait during the transition from the cold Late Glacial and into the warm early Holocene was elucidated via a multiproxy study of a marine sediment record retrieved at the western Svalbard slope. The multiproxy study includes analyses of planktic foraminiferal fauna, bulk sediment grain size and $CaCO_3$ content in addition to Mg/Ca ratios and stable isotopes ($\delta^{13}C$ and $\delta^{18}O$) measured on the planktic foraminifer *Neogloboquadrina pachyderma*. Furthermore paleo subsurface water temperatures were reconstructed via Mg/Ca ratios ($sSST_{Mg/Ca}$) and transfer functions ($sSST_{Transfer}$) enabling comparison between the two proxies within a single record. The age model was constrained by four accelerator mass spectrometry (AMS) ^{14}C dates.

From 14,000 to 10,300 cal yr B.P. *N. pachyderma* dominated the planktic fauna and cold polar sea surface conditions existed. The period was characterized by extensive sea ice cover, iceberg transport and low sub sea surface temperatures ($sSST_{Transfer}$ ~2.1°C; $sSST_{Mg/Ca}$ ~3.5°C) resulting in restricted primary production. Atlantic Water inflow was reduced compared to the present-day and likely existed as a subsurface current. At ca. 10,300 cal yr B.P. Atlantic Water inflow increased and the Arctic Front retreated north-westward resulting in increased primary productivity, higher foraminiferal fluxes and a reduction in sea ice cover and iceberg transport. The fauna rapidly became dominated by the subpolar planktic foraminifer *Turborotalita quinqueloba* and summer $sSST_{Transfer}$ increased by ~3.5°C. Concurrently, the $sSST_{Mg/Ca}$ recorded by *N. pachyderma* rose only ~0.5°C. From ca. 10,300 to 8,600 cal yr B.P. the average $sSST_{Mg/Ca}$ and $sSST_{Transfer}$ were ~4.0°C and ~5.5°C, respectively. The relatively modest change in $sSST_{Mg/Ca}$ compared to $sSST_{Transfer}$ can probably be tied to a change of the main habitat depth and/or shift in the calcification season for *N. pachyderma* during this period.

Keywords: Planktic foraminifera, Sub sea surface temperature reconstruction, Trace elements, Transfer functions, Stable isotopes, Late Glacial/Holocene transition, Fram Strait, Polar North Atlantic

1. Introduction

The Arctic region has responded strongly to both modern and past global climate changes (IPCC, 2007; Hald et al., 2007). One of the major components controlling the Arctic environment, including sea ice distribution, is the influx and volume of relatively warm and saline Atlantic Water flowing northwards into the Arctic Ocean (Schauer et al., 2004; IPCC, 2007). This influx primarily takes place through two gateways: the deep eastern Fram Strait (Schauer et al., 2004) and the shallower Barents Sea (Schauer et al., 2002). In order to improve our understanding of future climate changes in the Arctic region, it is a prerequisite to understand and quantify past rapid oceanic changes with regard to water volume transports, -temperature and -salinity.

Previous studies of the spatial and temporal oceanographic evolution in the Fram Strait show rapid changes through the Late Glacial – early Holocene transition. Atlantic Water masses were advected into the area during the Bølling-Allerød interstadial (Ślubowska et al., 2005; Ślubowska-Woldengen et al., 2007; Ebbesen et al., 2007; Rasmussen et al., 2007b), and during the Younger Dryas stadial the Atlantic Water advection continued submerged under a layer of polar surface water (Rasmussen et al., 2007b). During the early Holocene, advection of Atlantic Water was strong and it rapidly became dominant in the surface water masses (Ebbesen et al., 2007; Hald et al., 2007). These paleoceanographic reconstructions are based on a wide range of proxies, and with regard to estimation of past sea surface temperatures (SST) primarily stable isotopes measured in planktic foraminifera and transfer functions were used. Stable oxygen isotopes ($\delta^{18}O$) measured in foraminiferal

calcite inherently reflect the combined signal of salinity and temperature, while stable carbon isotopes ($\delta^{13}C$) reflect the degree of ventilation and primary production in the ambient water masses (e.g., Spielhagen and Erlenkeuser, 1994; Katz et al., 2010). Reconstructions of SST using transfer functions in the Arctic have been encumbered by several factors, including a restricted geographical distribution of the modern database (e.g., Kucera et al., 2005). Furthermore, it has been found that polar and subpolar planktic foraminifera migrate through the water column and have their maximum occurrence from 50 to 150 m water depth (e.g., Carstens et al., 1997; Volkmann, 2000). Husum and Hald (2012) used both annual and seasonal temperatures from different water depths and found the most robust statistical model using summer temperatures from 100 m water depth.

The aim of the present study is to improve qualitative and quantitative estimates of the paleoceanographic variability in the eastern Fram Strait during the transition from the Late Glacial into the early Holocene (14,000 - 8,600 cal yr B.P.). A multi proxy analysis was carried out using a sediment core retrieved from 1487 m water depth at the western Svalbard slope, eastern Fram Strait. We used stable isotopes ($\delta^{18}O$ and $\delta^{13}C$) measured on tests of *N. pachyderma*, planktic foraminiferal fauna distribution patterns, bulk sediment calcium carbonate ($CaCO_3$) content and grain size distributions to interpret the paleoceanography. In order to improve quantitative paleoceanographic reconstructions, we applied a transfer function by Husum and Hald (2012) to the downcore planktic foraminiferal fauna distribution, enabling reconstruction of summer subsurface temperatures ($sSST_{Transfer}$) (100 m water depth). Furthermore, paleo-subsurface temperatures were calculated from Mg/Ca ratios in *N. pachyderma* ($sSST_{Mg/Ca}$) which is an approach recently used in paleoceanographic reconstructions in the eastern Fram Strait (Spielhagen et al., 2011; Aagaard-Sørensen et al., 2013). Mg/Ca ratios of foraminifers primarily reflect water temperatures during test growth (e.g., Elderfield and Ganssen, 2000), while salinity and pH are subordinate influences on test

Mg uptake (Nürnberg et al., 1996; Lea et al., 1999). In the present study we use the species specific (*N. pachyderma*) Mg/Ca calibration by Kozdon et al. (2009) which enable temperature reconstructions of subpolar and polar water masses (>2.5°C). Foraminiferal test fragmentation was used to assess the pre-analytical preservation state of carbonates (Le and Shackleton, 1992; Pfuhl and Shackleton, 2004).

The investigated core site is situated under the axis of present-day inflow of Atlantic Water close to the Arctic Front dividing Atlantic and Arctic water masses (Fig. 1A) and is therefore well suited to record changes of the oceanic parameters within this main conduit of heat and salt to the Arctic. The time period from 14,000 to 8,600 cal yr B.P. was chosen for investigation as the rapid oceanographic changes previously documented across the Late Glacial-Holocene boundary (e.g., Ebbesen et al., 2007; Hald et al., 2007) may be construed as the most recent analogue to the rapid changes happening in the Arctic today (e.g. IPCC, 2007).

2. Oceanographic setting

The Fram Strait is a deep passage (2600 m) between Svalbard and Greenland that connects the north-eastern North Atlantic to the Arctic Ocean (Fig. 1A). Warm and saline Atlantic Water (T: 3 to 7°C; S: 34.9 to 35.2, Schauer et al., 2004; Walczowski et al., 2005) is transported towards the Arctic Ocean via the West Spitsbergen Current, a meridional branch of the North Atlantic Current (Loeng et al., 1997; Schauer et al., 2002) (Fig. 1A). The West Spitsbergen Current is topographically steered along the western slope of Spitsbergen through the eastern Fram Strait and into the Arctic Ocean (Blindheim and Rey, 2004; Walczowski et al., 2005). This makes the eastern Fram Strait the main pathway for heat and

salt advection into the Arctic Ocean (Schauer and Beszczynska-Möller, 2009). At present the water mass at the coring site is dominated by Atlantic Water occupying the upper 500 to 700 m of the water column below a ca. 25 m thick upper mixed layer (Fig. 1B). At ca. 78°N the advected Atlantic Water begins to submerge (e.g., Aagaard and Carmack, 1989) and a major part re-circulates in the Fram Strait creating a southward return flow, the Return Atlantic Water (RAW) (T: >0°C; S: >34.90) (Bourke et al., 1988) (Fig. 1). North of Svalbard Atlantic Water continues as a subsurface current into the Arctic Ocean northward as the Yermak Slope Current (Manley, 1995) and eastward as the Svalbard Branch along the northern continental slope of Svalbard (Aagaard et al., 1987; Manley, 1995) (Fig. 1A).

In the western part of the Fram Strait, the East Greenland Current occupies the upper ca. 150 m of the water column carrying a cold, low salinity (T: 0 to -1.7°C; S: ca. 30 to 34) polar water mass southward along with most (>90%) of the sea ice exported from the Arctic Ocean (Woodgate et al., 1999; Rudels et al., 1999, 2005)(Fig. 1A). In the central Fram Strait Polar and Atlantic Water mix and form Arctic Water masses with intermediate temperature and salinity (e.g., Hop et al., 2006). The contrasting water masses are separated by transition zones termed the Polar (separating Polar and Arctic water masses) and Arctic (separating Arctic and Atlantic water masses) Fronts which roughly define the average summer sea ice margin and the maximum limit of the winter sea ice margin, respectively (Swift and Aagaard, 1981; Hopkins, 1991) (Fig. 1A).

3. Material and methods

Kastenlot core MSM05/5-712-2 was retrieved from 1487 m water depth on the West Spitsbergen Slope in the eastern Fram Strait (78˚54.94’ N, 06˚46.04’ E) during a cruise of the

RV *Maria S. Merian* in August 2007 (Fig. 1A). Water conductivity, temperature, and depth were measured prior to coring (Fig. 1B). Proxy data from the 8.94 m long sediment core are presented here at the core depth interval from 209 to 441cm. The interval is constrained by four previously published accelerator mass spectrometry (AMS) radiocarbon date measurements (Fig. 2) (Aagaard-Sørensen et al., 2013). Due to low abundance of planktic foraminifera in the sediment below ca. 330 cm core depth it was only possible to collect enough material for one AMS date. Therefore, the age model below this point is poorly constrained. The AMS measurements were performed at the Leibniz Laboratory of Kiel University, Germany, and Poznań Radiocarbon Laboratory, Poland (Table 1). Calibration of the radiocarbon dates was performed using Calib version 6.0 (Reimer et al., 2004; Stuiver et al., 2005) and the marine calibration curve Marine09 (Hughen et al., 2004; Reimer et al., 2009). A total reservoir age of 551±51 years was used. This value was reached using the standard reservoir correction of 400 years and the modern reservoir age (ΔR) of 151 ± 51 years from the nearby Magdalenafjorden (Mangerud and Gulliksen, 1975; Mangerud et al., 2006). The age model was established by linear interpolation between the calibrated radiocarbon dates using the mean of the 2σ interval of highest probability as individual tie points (Fig. 2, Table 1). In figures and text all dates will refer to calibrated years before present, B.P. (present=1950). The Late Glacial - Holocene chronostratigraphic zones are based on the most recent divisions defined on the basis of Greenland ice cores (Rasmussen et al., 2006, 2007a; Steffensen et al., 2008; Walker et al., 2009): Bølling-Allerød interstadial 14,650 to 12,850 cal yr B.P., Younger Dryas 12,850 to 11,650 cal yr B.P. and Holocene 11,650 cal yr B.P. to present.

The lithology of the sediment core was visually described onboard after coring. Sediment samples, at 6 cm-intervals, were freeze-dried and wet-sieved through 63 µm, 100 µm and 1 mm sieves. Dried sample fractions were weighed and used to determine the grain

size distribution. The >1 mm size fraction is considered as ice-rafted debris (IRD) (Fig. 3). Total organic carbon (TOC) and total carbon (TC) were measured using a Leco CS 200 furnace at the University of Tromsø. The TC content (wt.%) was measured directly on bulk sediment samples while the TOC content (wt.%) was measured on samples pre-treated with HCl (10%) to remove $CaCO_3$ before combustion (1350ºC). Subsequently bulk sediment $CaCO_3$ content was calculated using the equation: $CaCO_3$ = (TC-TOC)*100/12 (e.g., Knies et al., 2003) (Fig. 3). $CaCO_3$ from 11,700 to 8,600 cal yr B.P. have previously been published in Aagaard-Sørensen et al. (2013).

Approximately 300 planktic foraminifer specimens picked from the 100 µm-1 mm size fraction were identified to species level and relative foraminiferal distributions and fluxes were calculated (Fig. 3). Transfer function summer (July to September) sub sea surface temperatures ($sSST_{Transfer}$) at 100 m water depth were reconstructed using the C.2 program (ver 1.6) (Juggins, 2010) (Fig. 5). The applied transfer function is based on a training set consisting of modern planktic foraminifera picked from the 100-1000 µm size fraction in northern North Atlantic core top sediments and the Weighted Average Partial Least Square (WAPLS) model (Husum and Hald, 2012). For the $sSST_{Transfer}$ reconstruction the three component WAPLS model cross-validated by "jack knifing" was used. This model produced low root mean squared error (RMSE) and low maximum bias in conjunction with relatively high correlation between observed and estimated values (r^2) (e.g., Ter Braak and Juggins,1993; Birks, 1995; Husum and Hald, 2012) (Table 2). Planktic foraminiferal test fragments picked from the 100-1000 µm size fraction were counted and a fragmentation index was calculated using the equation of Pfuhl and Shackleton (2004): Fragmentation (%) = # fragments * 100 / (# tests * (1/3 * # fragments)) (Fig. 4). Visual inspection of samples and the structure of the broken fragments lead us to assume that tests broke down into

multiple fragments. Therefore, we applied a fragment-divisor of 3 (Le and Shackleton, 1992; Pfuhl and Shackleton, 2004).

Stable isotope measurements were performed at the GEOMAR Helmholtz Centre for Ocean Research, Kiel using a Finnigan MAT 253 mass spectrometer (reproducibility of ±0.03‰ for $\delta^{13}C$ and ±0.06‰ for $\delta^{18}O$) and a Kiel IV Carbonate Preparation Device. Stable oxygen and carbon isotopic ratios were measured on 20 to 30 tests of the planktic foraminifer species *N. pachyderma* picked from the 125-250 μm sieve size fraction (Fig. 4). In order to use well-mixed aliquots the tests were crunched and mingled. All measurements were calibrated to Vienna Pee Dee Belemnite (VPDB) standard (NBS 19). Measurements were carried out at 1 cm-intervals apart from at 373-380 cm core depth where scarcity of foraminiferal fauna prevented analysis. The $\delta^{18}O$ isotope record was not corrected for vital effects (Jonkers et al., 2010) but for the ice volume effect (Fairbanks, 1989) (Fig. 4). For comparison we also show the uncorrected $\delta^{18}O$ isotope record and the record corrected for the ice volume effect according to the ICE-5G(VM2) model (Peltier and Fairbanks, 2006) (Fig. 4).

Trace element analysis was performed every 3 cm on ca. 50 tests of *N. pachyderma*. Specimens were picked at a narrow size fraction (225-290 μm) to minimize possible size-dependent bias (Elderfield et al., 2002). Foraminiferal tests were gently crushed between glass plates to expose all test chambers to the reductive (anhydrous hydrazine) and oxidative (H_2O_2) cleaning procedures following Boyle and Keigwin (1985) and Boyle and Rosenthal (1996). Cleaned samples were analyzed for Mg/Ca, Mn/Ca and Fe/Ca by magnetic-sector single-collector ICP-MS, on a Thermo-Finnigan Element2 at INSTAAR, University of Colorado (Marchitto, 2006). Standards, with minor and trace element concentrations that mimic the typical oceanic ranges of foraminifera, were prepared gravimetrically using 1000 ± 3 mg L11 stock solutions from High-Purity Standards and SPEX CertiPrep and made at 5

mM (200 ppm) Ca in 2% (v/v) HNO_3 (Fisher Optima) (Marchitto, 2006).^{26}Mg, ^{55}Mn and ^{56}Fe were measured in analog mode and ratioed to ^{43}Ca in low (Mg, Mn) and medium (Fe) resolution (Marchitto, 2006). Replicate analysis was performed for every ca. 20th sample. The average Mg/Ca reproducibility of sample splits was ±0.049 mmol/mol (n=3) which is below 4% difference between the average and recorded duplicate values. The system has long-term 1σ precisions for Mg/Ca of 0.5% (Marchitto, 2006). Samples with >100 µmol/mol in regards to Fe/Ca (n=3) or Mn/Ca (n=4) were omitted (Fig. 4) due to possible contamination by detrital material or secondary diagenetic coatings, which could lead to biased Mg/Ca values (Barker et al., 2003). Likewise one sample with <5µg $CaCO_3$ postcleaning mass was omitted (Marchitto, 2006) (Fig. 4). Foraminiferal Mg/Ca ratios measured from 11,700 to 8,600 cal yr B.P. have previously been published in Aagaard-Sørensen et al. (2013).

Mg/Ca thermometry was used to obtain quantitative reconstructions of sea surface temperatures ($SST_{Mg/Ca}$) by applying a species-specific (*N. pachyderma*) temperature equation (Fig. 5). The applied linear equation of Kozdon et al. (2009) is based on cross calibrated Mg/Ca and $\delta^{44/40}$Ca proxy signals of *N. pachyderma* in Holocene core top samples from the Nordic Seas: Mg/Ca (mmol/mol) = 0.13(±0.037) * T (°C) + 0.35(±0.17), where numbers in parentheses show the error margins. Despite exponential thermodynamic control on Mg uptake in calcareous foraminiferal tests this equation assumes that linearity adequately depicts the Mg uptake/temperature relation in the narrow temperature range inhabited by *N. pachyderma* and works for reconstructed temperatures above ca. 2.5°C (Mg/Ca >0.74 mmol/mol) (Kozdon et al., 2009). However, when temperatures are lower than 2.5°C, which is typically associated with salinities less than 34.5, the method loses its precision (Kozdon et al., 2009). The reductive cleaning of foraminiferal calcite utilized in the present study has been shown to potentially decrease the Mg/Ca ratio by up to 15 % (Barker et al., 2003). For comparison and in order to evaluate the potential impact of the reductive cleaning on the

239 temperature reconstructions we artificially increased the Mg/Ca ratio by 15% before
240 recalculating $sSST_{Mg/Ca}$ (Fig. 5) (See Discussion).
241
242 **4. Results**

243 **4.1 Lithology**

244 The sediment comprises two different lithological units. Unit B (14,000 - 10,300 cal
245 yr B.P.; 442 – 323 cm) holds dark olive grey monosulphide-rich silty clay with ca. 1 cm thick
246 olive black laminations. The overlying unit A (10,300 - 8,600 cal yr B.P.; 323 – 208 cm)
247 holds dark homogeneous olive grey, monosulphide-rich bioturbated silty clay (Fig. 3). The
248 sedimentation rate of unit B is 32 cm/kyr vs. 59 to 108 cm/kyr in unit A (Fig. 2). Unit B holds
249 2 to 7 wt.% material >63 µm (Fig. 3) and up to 4 wt.% material >1 mm (IRD) (Fig. 3). Two
250 periods at 13,300 - 12,200 and 11,500 - 10,900 cal yr B.P. hold higher concentrations of
251 material >1 mm averaging 2 wt.%. Unit A is very fine grained with ~98 wt.% of material <63
252 µm. A diatom rich layer was identified at 10,500 - 9,800 cal yr B.P. (329 – 281 cm) (Fig. 3).
253 $CaCO_3$ values were low, averaging 4.5 wt.% prior to 10,000 cal yr B.P., and increased from
254 ca. 5 to 13 wt.% during the succeeding 1400 years (Fig. 3).

255 **4.2 Planktic foraminifera, Transfer function sSST and shell fragmentation**

256 Polar and subpolar species *N. pachyderma* and *Turborotalita quinqueloba* dominate
257 the planktic foraminiferal fauna (Figs. 3, 5). The clear dominance of these two species is
258 characteristic for Arctic marine environments (e.g., Johannessen et al., 1994; Carstens et al.,
259 1997; Volkmann, 2000). Between 14,000 to 10,500 cal yr B.P. the faunal fluxes were low
260 (ca. 2 specimens/cm^2*yr) (Fig. 3) and the foraminiferal fauna was dominated by *N.*
261 *pachyderma* (>86%) with *T. quinqueloba* and *Neogloboquadrina incompta* (formerly denoted
262 *N. pachyderma* (dextral coiling); Darling et al., 2006) as secondary species (<10%).

263 Between 10,500 and 10,100 cal yr B.P. *T. quinqueloba* became the dominant species
264 coincident with increasing planktic foraminifer fluxes (Figs. 3, 5). Relative abundance of *T.*
265 *quinqueloba* averaged 63% from 10,100 to 8,600 cal yr B.P., while overall planktic fluxes
266 remained high averaging 50 specimens/cm^2*yr. In this period *N. pachyderma* constituted ca.
267 25% of the total fauna except at ca. 8,800 cal yr B.P. where it reached 68% (Fig. 3). After
268 10,500 cal yr B.P. other commonly found species were *N. incompta* (ca. 6%), *Globigerina*
269 *bulloides* (>3.1%), *Globigerinita calida* (>2.4%), *Globigerinita glutinata* (>2.2%) and
270 *Globigerinita uvula* (up to ca. 10%). *Globigerinita uvula* was primarily present from 10,000
271 to 9,200 cal yr B.P. with a peak in relative abundance of ca. 10% at 9,900 cal yr B.P. (Fig. 3).

272 The sub sea surface temperatures obtained by transfer functions ($sSST_{Transfer}$) show
273 low values ranging from 1.9 to 2.7°C (average 2.1°C) prior to ca. 10,300 cal yr B.P. A rapid
274 temperature increase occurred between ca. 10,500 to 10,100 cal yr B.P. followed by relatively
275 high, but slowly declining, temperatures ranging from 3.3 to 6.5°C (average 5.5°C) from
276 10,100 to 8,600 cal yr B.P. (Fig 5).

277 Low fragmentation of planktic foraminiferal tests, averaging 3.4% was found from
278 14,000 to 12,850 cal yr B.P. (Fig. 4). From 12,850 to 10,500 cal yr B.P. values were
279 generally higher, averaging 13.8% with values exceeding 45% around 12,000 cal yr B.P.
280 From 10,500 to 8,600 cal yr B.P. values averaged 8.9% with the highest value (32.2%) at ca.
281 8,800 cal yr B.P.

282 **4.3 Stable isotopes**

283 *N. pachyderma* $\delta^{13}C$ values show two local maxima at ca. 12,700 (0.25‰) and ca.
284 8,800 cal yr B.P. (0.45‰) in addition to a broad maximum at 11,600 - 10,200 cal yr B.P.
285 (average ca. 0.25‰) (Fig. 4). Low average values of ca. 0.1‰ were found at 10,200 - 9,000
286 cal yr B.P.

N. pachyderma $\delta^{18}O$ values increased from ca. 3.1‰ at 14,000 to 3.7‰ at 12,100 cal yr B.P. (Fig. 4). Low average values (around 2.9‰) from 11,900 to 11,500 cal yr B.P. were followed by an increase leading to values of ca. 3.5‰ at ca. 11,400 - 11,200 cal yr B.P. From ca. 11,000 cal yr B.P. the values declined and reached a minimum at ca. 9,500 cal yr B.P. (ca. 2.5‰) with one marked excursion towards heavier values at ca. 10,000 cal yr B.P. A slightly increasing trend was observed after 9,500 cal yr B.P. (Fig. 4).

4.5 Mg/Ca ratios and reconstructed $SST_{Mg/Ca}$

The Mg/Ca ratios show values ranging from ca. 0.6 to 1.07 mmol/mol in the analysed interval. An overall slightly increasing trend is noticed towards the youngest part of the record (Fig. 4). Highest values were found at ca. 13,200, ca. 11,600 and after ca. 10,300 cal yr B.P. Average Mg/Ca values were 0.81 mmol/mol prior to and 0.86 mmol/mol after 10,300 cal yr B.P. (Fig. 4). Sea surface temperatures based on Mg/Ca ratios ($SST_{Mg/Ca}$) (equation by Kozdon et al., 2009) show temperature fluctuations between ca. 2.5 and 5.5°C throughout the record. Average temperatures are 3.5ºC before and 4.0ºC after 10,300 cal yr B.P. (Fig. 5).

5. Discussion

5.1. Evaluation of proxies

In the present study paleoceanography and paleo-water temperature in the eastern Fram Strait across the Late Glacial – early Holocene transition was estimated and reconstructed via Mg/Ca ratios and stable isotopes in *N. pachyderma*, fossil foraminiferal fauna, and chemical and physical properties of the sediment (Figs. 3, 4, 5).

N. pachyderma reflects/records ambient water properties at varying depths below the thermocline from ca. 25-250 m water depth (e.g., Simstich et al., 2003) where modern day temperature (August 2007) is 3.7-6.7°C and salinity is ~35.1 (Fig. 1B). Therefore water mass

property reconstruction, via stable isotopes and trace elements on this biotic carrier, do not reflect actual sea surface conditions and in the following discussion $SST_{Mg/Ca}$ is denoted as sub SST ($sSST_{Mg/Ca}$).

Low fluxes of planktic foraminifera and dominance of *N. pachyderma* (>90%) characterized the period prior to 10,300 cal yr B.P. (Fig. 3). From 14,000 to 12,800 cal yr B.P., the fragmentation of tests was low indicating good preservation (Fig. 4). From ca. 12,800 to 10,500 cal yr B.P., fragmentation was elevated, indicating reduced test preservation (Le and Shackleton, 1992; Pfuhl and Shackleton, 2004) (Fig. 4). Highest fragmentation was observed around 12,000 cal yr B.P. indicating that the test preservation was at a minimum for the record as a whole (Fig. 4). This may have contributed to the scarcity of planktic foraminifera observed at this time, leading to a deficient number of specimens for stable isotope analysis (Figs. 3, 4). In addition, the only sample from the trace element dataset omitted due to low post-cleaning mass refers to this approximate age potentially suggesting that the foraminiferal calcite had been exposed to pre-analytic dissolution (Fig. 4). Barker et al. (2005) found that low test preservation (i.e., enhanced dissolution) generally causes a lowering of Mg/Ca ratios in foraminiferal calcite and thereby lowers the temperature estimates. Furthermore, reduced preservation of planktic foraminiferal tests could facilitate selective removal/destruction of dissolution-prone species (e.g. *T. quinqueloba*, *G. uvula*) from the fossil assemblages (e.g., Conan et al., 2002). This can result in a relative increase in dissolution-resistant species (e.g., *N. pachyderma*) and modification of the faunal composition (e.g., Conan et al., 2002; Zamelczyk et al., 2012). Despite the difference in fragmentation between the two periods (14,000 - 12,800 and 12,800 - 10,500 cal yr B.P.), no distinct change in Mg/Ca ratios or fauna composition was observed (Figs. 3, 4). This indicates that the preservation of tests had little or no impact on the present sSST reconstructions (Fig. 5).

Barker et al. (2003) found that the reductive cleaning of foraminiferal calcite used in the trace element analysis (see Material and methods section for details) potentially decreases the Mg/Ca by up to 15%, thereby lowering the reconstructed $sSST_{Mg/Ca}$. Prior to ~10,500 cal yr B.P. the $sSST_{Mg/Ca}$ reconstruction shows temperatures that were larger than the $sSST_{Transfer}$ (Fig. 5). By artificially increasing the Mg/Ca ratios by 15% the resulting temperature estimates become even higher (~1°C) tentatively suggesting that the reductive cleaning procedure is of minor importance for the reconstructed $sSST_{Mg/Ca}$ (Fig. 5). This tentative conclusion is supported by earlier studies from the same core site that include Mg/Ca temperature reconstructions based on the same biotic carrier (*N. pachyderma*) and the same exact cleaning procedure as the material in the present study (Spielhagen et al., 2011; Aagaard-Sørensen et al., 2013). Spielhagen et al. (2011) showed minor difference between measured modern water temperatures and core-top $sSST_{Transfer}$ and $sSST_{Mg/Ca}$, while comparison of reconstructed summer $sSST_{Transfer}$ published by Werner et al. (2013) with $sSST_{Mg/Ca}$ from 8,800 cal yr B.P. to the present within the upper part of core MSM05/5-712-2 showed similar temperature ranges (Aagaard-Sørensen et al., 2013).

Prior to the Holocene Arctic surface water masses were spread far to the south and east in the northeastern North Atlantic (Koç et al., 1993) and thus could have influenced the coring site. Kozdon et al. (2009) found that modern Mg/Ca-derived temperature estimates from the cold (<3ºC), low saline Arctic domain and Polar waters in the Nordic Seas were higher than corresponding maximum SST in the areas. Therefore it must be cautioned that our $sSST_{Mg/Ca}$ reconstruction, with values averaging 3.6ºC prior to ~10.500 cal yr B.P., could potentially be erroneously high (Fig. 5). The fact that the average value of $sSST_{Mg/Ca}$ is higher than average value of $sSST_{Transfer}$ in this period could alternatively suggest that $sSST_{Mg/Ca}$ measured on *N. pachyderma* reflect another water depth than the water depth represented by the $sSST_{Transfer}$ reconstruction. While the $sSST_{Transfer}$ values reflect temperatures at 100 m

water depth (Husum and Hald, 2012), $sSST_{Mg/Ca}$ may reflect shallower water depths where temperatures presumably were higher (Fig. 5). The depth habitats of *N. pachyderma* have been found to be shallower than 100 m water depth in Arctic areas influenced by sea ice (Volkmann, 2000; Simstich et al., 2003; Pados and Spielhagen, in press). These findings may therefore suggest that the calcification depth of *N. pachyderma* was shallower than 100 m in the period from ca. 14,000 - 10,500 cal yr B.P.

In addition, the observed difference between the $sSST_{Transfer}$ and $sSST_{Mg/Ca}$ reconstructions may be linked to seasonal differences between the proxy approaches. In the Arctic region peak fluxes of planktic foraminifera are reported during summer at sea ice margins with high primary production (Carstens et al., 1997). Thus, during periods with ice-cover and abundant icebergs, like the earliest part of our record (see section 5.2 for further discussion), the primary production bloom and calcification season of *N. pachyderma* (i.e. $sSST_{Mg/Ca}$) was possibly delayed/shifted towards late summer where water temperatures potentially were higher than the average summer (July to September) temperatures reconstructed by the transfer functions ($sSST_{Transfer}$) (Fig. 5).

After ~10,300 cal yr B.P., the subpolar species *T. quinqueloba* became the dominating species (average >60%) and the flux of planktic foraminifera increased markedly (Figs. 3, 5). The species *T. quinqueloba* is prone to dissolution, so when it is found in high numbers together with relatively low test fragmentation, the test preservation is good (Figs. 3, 4). Average $sSST_{Mg/Ca}$ values from 10,300 to 8,600 cal yr B.P. were ~0.5°C higher compared to the previous period (14.000 to 10.300 cal yr B.P.) (Fig. 5). This finding is in contrast to summer $SST_{Transfer}$ reconstructions from the Norwegian–Svalbard margin where average values at 10 m water depth rose ~5°C in the early Holocene (Hald and Aspeli, 1997; Ebbesen et al., 2007; Hald et al., 2007). However, when applying the transfer function of Husum &

Hald (2012) reconstructing temperatures for subsurface water masses at 100 m water depth for the new and the abovementioned records a temperature increase of ~3.5°C is generated in this period (Fig. 5). During most of the early Holocene the $sSST_{Transfer}$ (100 m water depth) remains higher than $sSST_{Mg/Ca}$ suggesting that *N. pachyderma* may have responded to oceanographic changes by descending in the water column and calcifying at depths below 100 m (Fig. 5).

Kozdon et al. (2009) suggest that *N. pachyderma* throughout its life cycle is actively or inactively linked to an isopycnal layer with densities (σ_t) ranging from 27.7 to 27.8, corresponding to a depth of 60-110 meters with the present day temperature and salinity profile (Fig. 1B). As a consequence the species prefers gradually deeper habitats with increasing temperatures, thus counterbalancing absolute sea surface temperature variations (Kozdon et al., 2009). This suggestion could explain the relatively narrow (ca. 2.5 to 5.5°C) temperature range depicted by the $sSST_{Mg/Ca}$ reconstruction (Fig 5) during a period and in a region where significant oceanographic changes have been described (e.g. Koç et al., 2002; Hald et al., 2007; Rasmussen et al., 2007b; Ebbesen et al., 2007; Farmer et al., 2008). However, numerous studies showed that factors such as sea ice cover, proximity to sea ice margins and oceanic fronts, water column stratification, water mass distribution, and food availability also can influence the habitat depth of planktic foraminifera (Carstens et al., 1997; Volkmann, 2000; Simstich et al., 2003; Jonkers et al., 2010). Furthermore, a recent comparison of plankton tow and physical oceanography data from the Fram Strait has shown that the link of the *N. pachyderma* habitat to a narrow isopycnal band is less distinct in ice-covered than in ice-free waters (Pados and Spielhagen, in press).

As mentioned earlier seasonal changes in calcification of *N. pachyderma* can also impact the $sSST_{Mg/Ca}$ values. In the central Irminger Sea (~59°N) Jonkers et al. (2010) reports largest fluxes of *N. pachyderma* during spring and in late summer, when SSTs can be

relatively variable. The strongly fluctuating $sSST_{Mg/Ca}$ in the early Holocene could therefore also result from shifts in calcification season of *N. pachyderma* (Fig. 5). Moreover, laboratory experiments have shown fastest growth rates for *N. pachyderma* at temperatures around 5°C, and growth rates progressively slowing with increasing temperatures (Lombard et al., 2009). This suggests that *N. pachyderma*, during the early Holocene, may have calcified earlier in the season, when temperatures were more favorable (Fig. 5).

5.2. Paleoenvironmental reconstruction and correlation

5.2.1 Period: 14,000 to 12,850 cal yr B.P. (Bølling-Allerød interstadial)

The Bølling-Allerød interstadial is characterized by a planktic foraminiferal fauna assemblage dominated by *N. pachyderma* (>90%) that together with low faunal fluxes, and low $CaCO_3$ indicate polar conditions with reduced productivity (Johannessen et al., 1994) (Fig. 3). This is supported by the reconstructed $sSST_{Transfer}$ showing cold summer conditions (averaging 2°C) throughout the period (Fig. 5). Previous studies have documented relatively strong meridional advection of Atlantic Water through the Eastern Fram Strait during Bølling-Allerød (Birgel and Hass, 2004; Ślubowska et al., 2005; Rasmussen et al., 2007b). The concurrent higher $sSST_{Mg/Ca}$ (averaging 3.5°C) could therefore suggests that *N. pachyderma* calcified in chilled Atlantic Water masses, likely at water depths above 100 m and during peak (late) summer conditions during this period (Fig. 5) (see 5.1. Evaluation of proxies for further discussion).

Relatively large amounts of sand (>63 µm) and IRD (>1 mm) show influence of icebergs and coastal sea ice at the core site, while low $\delta^{13}C$ values indicate stratification (e.g., Spielhagen and Erlenkeuser, 1994) which probably was caused by sea ice and melt water (Figs. 3, 4). Low $\delta^{13}C$ values are also recorded further south at ca. 77°N in the Fram Strait

(Ebbesen et al., 2007) and at ca. 75°N on the Barents Sea slope (Sarnthein et al., 2003) during this period. The two IRD peaks found at around 13,600 and 13,100 cal yr B.P. may correlate with cold inter Bølling-Allerød periods recorded in the NGRIP ice core (Rasmussen et al., 2006) (Fig. 5). This suggests increased calving, transport and melting of icebergs or sea ice during periods with cold atmospheric conditions. Elevated coarse fraction and IRD concentrations have previously been reported during Bølling-Allerød on the West Spitsbergen Slope (Rasmussen et al., 2007b; Ebbesen et al., 2007; Jessen et al., 2010), while concurrent decreased IRD concentrations were ascribed to more prolonged and severe sea ice conditions north of Svalbard under the axis of the Svalbard Branch (Fig. 1) (Koç et al., 2002; Ślubowska et al., 2005).

5.2.2 Period: 12,850 to 11,650 cal yr B.P. (Younger Dryas)

During Younger Dryas the planktic foraminiferal assemblage was dominated by *N. pachyderma* (>90%) indicating cold polar sea surface conditions (Fig. 3) (Johannessen et al., 1994). The sediment $CaCO_3$ content and flux of planktic foraminifera were also low, pointing at continued reduced primary production in the water column (Fig. 3). Slightly lowered sand (>63µm) and IRD concentrations during this period (Fig. 3) may be interpreted as either increased sea ice cover that suppressed iceberg transport, decreased glacier calving on Svalbard and/or surface waters that were too cold to allow melting of icebergs/sea ice. Low IRD concentrations west and north of Svalbard have previously been linked to prolonged sea ice coverage and reduced iceberg transport during the Younger Dryas (Koç et al., 2002; Wollenburg et al., 2004; Ebbesen et al., 2007; Ślubowska-Woldengen et al., 2007). Cold conditions during the Younger Dryas stadial have been documented in numerous proxy records in the Arctic region including ice core records (e.g. Rasmussen et al., 2006) (Fig. 5), terrestrial proxy records (e.g. Landvik et al., 1998), and marine proxy records (e.g. Koç et al., 1993; Ślubowska-Woldengen et al., 2007; 2008).

During the early part of the Younger Dryas (~12.800 – 12.000 cal yr B.P.) continued low $sSST_{transfer}$ (averaging 2°C) and lowered $sSST_{Mg/Ca}$ (averaging 3.2°C) combined with high $\delta^{18}O$ show that cold summer conditions prevailed while chilled Atlantic Water remained present during the foraminiferal growth season (Figs. 4, 5). This is supported by Rasmussen et al. (2007b) who found that subsurface advection of Atlantic Water to the Fram Strait continued and that the water mass was colder and probably less saline than during the preceding Bølling-Allerød.

Increased freshwater injections and sea ice expansion in the Nordic Seas have previously been identified and linked to hampered meridional overturning circulation during the Younger Dryas (e.g., Broecker et al., 1989; Koç et al., 1993; Sarnthein et al., 1995; Hald and Aspeli, 1997; Jennings et al., 2006; Bradley and England, 2008). The almost foraminiferal-barren/high fragmentation interval (~12,100 to 11,900 cal yr B.P) and subsequent low $\delta^{18}O$ values may indicate increased freshwater influence in the surface and subsurface water mass at ca. 12,100 to 11,500 cal yr B.P. (Fig. 3, 4). However, following the period with high fragmentation/low test preservation at the end of Younger Dryas and into the Preboreal (11,900 - 11,500 cal yr B.P.) the somewhat elevated average $sSST_{Mg/Ca}$ (~4°C) could alternatively suggest that the lowered $\delta^{18}O$ may be interpreted as a temperature increase during the season and/or at the depth of *N. pachyderma* calcification (Figs. 4, 5).

5.2.3 Period: 11,650 to 8,600 cal yr B.P. (Early Holocene)

In the earliest part of the Holocene, until ca. 10,500 cal yr B.P., cold surface water conditions, with a low flux foraminiferal fauna dominated by *N. pachyderma*, continued (Fig. 3). The sand and IRD content rose slightly, showing a continued, possibly enhanced, influence of sea ice and iceberg melting (Fig. 3). Similar, cold sea and sea ice/iceberg-influenced surface conditions are recorded both west and north of Svalbard during this period (Ebbesen et al.,

2007; Ślubowska-Woldengen et al., 2007). The marked IRD peak observed at ca. 11,000 cal yr B.P. (Fig. 3) correlates to rapid ice retreat on Svalbard and in western Barents Sea (Landvik et al., 1998). Despite the apparent continued influence from sea ice and icebergs in the area, the average $\delta^{13}C$ value was higher than during Younger Dryas, suggesting improved ventilation of the water mass (cf. Spielhagen and Erlenkeuser, 1994). Alternatively the higher $\delta^{13}C$ values could reflect increased primary production (e.g., Katz et al., 2010) in the surface waters, which is tentatively supported by the slightly elevated planktic foraminiferal fluxes (Figs. 3, 4).

After ~11,500 cal yr B.P., the $\delta^{18}O$ values steadily decreased until ~9.700 cal yr B.P. indicating gradually lowered salinity and/or increased temperatures within the sub surface water mass (Fig. 4). The reconstructed $sSST_{Mg/Ca}$, although strongly fluctuating, show a concurrent increasing trend, supporting the latter interpretation of the $\delta^{18}O$ signal (Fig. 5). A similar declining $\delta^{18}O$ trend is also observed on the south-western Svalbard slope (76°N) (Rasmussen et al., 2007b) and on the western Barents Sea shelf (75°N) (Sarnthein et al., 2003) at this time, indicating increasing northward heat advection via the Norwegian Atlantic Current (NwAC), suggested by Risebrobakken et al. (2011) to have culminated at ~10,000 cal yr B.P.

The generally decreasing $\delta^{18}O$ trend is punctuated by several excursions towards heavier values with most pronounced increases >0.5‰ observed at ~11,300 and 10,000 cal yr B.P. (Fig. 4) that are likely related to short term regional cooling events. The cooling at ~11,300 cal yr B.P. correlates to the Preboreal Oscillation cooling event, which has been observed in various marine proxy records in the Fram Strait, Nordic Seas and in northern Norway (e.g., Björck et al., 1997; Hald and Hagen, 1998; Husum and Hald, 2002; Ślubowska et al., 2005) and in Greenland ice cores (Rasmussen et al., 2006, 2007a) (Fig. 5) while the

latter (~10.000 cal yr B.P) approximately correlates to the so-called 9.95 ka anomaly (presented on the b2k scale) in the Greenland ice cores (Rasmussen et al., 2007a). However, the lower resolution of the $sSST_{Mg/Ca}$ and $sSST_{Transfer}$ records does not merit confirmation that these $\delta^{18}O$ excursions represent coolings (Figs. 4, 5).

The transition from the cold Younger Dryas stadial to the warm Holocene interglacial has been recorded in Greenland ice core records at 11,650 cal yr B.P. (Rasmussen et al., 2006; Walker et al., 2009) (Fig. 5). Associated with a northward displacement of the Arctic Front, separating Arctic and Atlantic water masses, Hald et al. (2007) showed that surface water masses in the eastern part of the Nordic Seas experienced a time-transgressive transition from cold Late Glacial into warm Holocene sea surface conditions. The transition happened at ca. 11,800 cal yr B.P. at 60°N and at ca. 10,500 cal yr B.P. at 77°N (Hald et al., 2007 and ref therein). In areas north of 71°N the rise in transfer function-reconstructed SST was primarily driven by a rapid increase in *T. quinqueloba* abundances (Hald and Aspeli, 1997; Ebbesen et al., 2007; Hald et al., 2007) (Fig. 5). A rapid increase in abundance and flux of *T. quinqueloba* can also be observed in our record, translating into a $sSST_{Transfer}$ increase of ~3.5°C between 10,500 to 10,200 cal yr B.P. (Fig. 5). The timing of this rapid increase is in accordance with the northward delay in onset of warmer surface conditions observed by Hald et al. (2007) in the Nordic Seas. The delayed Holocene oceanic warming at high latitudes has been attributed to the lingering impact of a cold water and sea ice pool in high Arctic settings (Hald et al., 2007) which at our core site is expressed as coarser and more IRD laden sediment deposited before ~10,500 cal yr B.P. (Fig. 3). The delayed warming has furthermore been connected to high albedo caused by sea ice/snow cover and the related asymmetry of atmospheric and oceanic circulation patterns (e.g., Kaufman et al., 2004).

The faunal transition was also associated with increased abundance and flux of the relatively thermophile species *N. incompta* and *G. bulloides* indicating stronger influence from Atlantic Water (Johannessen et al., 1994; Risebrobakken et al., 2011) in the eastern Fram Strait with summer $sSST_{Transfer}$ averaging ca. 5.5°C after ca. 10,300 cal yr B.P. (Figs. 3, 5). This change coincides with markedly increased bottom current speeds in the northern Fram Strait (Birgel and Hass, 2004) and strong inflow of Atlantic Water to the western and northern Svalbard margin and fjords (Ślubowska-Woldengen et al., 2007; Skirbekk et al., 2010). The increased Atlantic Water influx likely also led to cessation of iceberg transport, as indicated by absence of IRD in our record after ca. 10.500 cal yr B.P. (Fig. 4B) which occurred almost concurrently all along the West Spitsbergen Slope (Ebbesen et al., 2007; Rasmussen et al., 2007b; Jessen et al., 2010).

The high flux and abundance of *T. quinqueloba* combined with generally increased planktic foraminiferal fluxes and increasing sediment $CaCO_3$ content after ca. 10,300 cal yr B.P. (Figs. 3, 5) shows that the Arctic Front and associated productive water masses probably were situated close to the west Spitsbergen and Barents Sea slopes during the early Holocene (Johannessen et al., 1994; Hald and Aspeli, 1997; Sarnthein et al., 2003; Ebbesen et al., 2007). A pronounced peak in relative percentage and flux of *G. uvula*, a species that tolerates lowered salinities and is found in cold productive surface waters near oceanic fronts (Boltovskoy et al., 1996; Husum and Hald, 2004) is observed at ca. 10,000 to 9,300 cal yr B.P. (Fig. 3). High concentration of diatom frustules have been found in the sediments all along the West Spitsbergen Slope during the Early Holocene (Jessen et al., 2010) and is also observed in the present record between ca. 10,500 to 9,800 cal yr B.P. (Fig. 3). In conjunction with the presence of *G. uvula* this finding further indicates the presence of highly productive water masses in the area which likely was linked to proximity of the Arctic Front during the Early Holocene (Fig. 3).

After ca. 10,000 cal yr B.P. minimum $\delta^{18}O$ values together with somewhat elevated average $sSST_{Mg/Ca}$ (~4°C) indicate that ambient water temperatures during *N. pachyderma* test formation were the highest within the record (Figs. 4, 5), while relatively low $\delta^{13}C$ values indicate that the water mass was less ventilated at ca. 10,500 to 9,000 cal yr B.P. (Fig. 4). The warm conditions are also reflected by the high summer $sSST_{Transfer}$ (averaging ~5.5°C) recorded after 10,300 cal yr B.P. (Fig. 5). However, the $sSST_{Transfer}$ shows a trend toward lower average summer temperatures after ca. 9,300 cal yr B.P. with a pronounced low (~3.3°C) observed at ca. 8,800 cal yr B.P. (Figs. 4, 5), which may indicate the first step towards the termination of high early Holocene summer surface temperatures also observed in other records along the Barents Sea and West Spitsbergen slopes at approximately this time (Sarnthein et al., 2003; Ebbesen et al., 2007).

6. Conclusions

The paleoceanographic reconstruction shows polar surface conditions with faunal dominance of the polar species *N. pachyderma* in the study area from 14,000 to 10,300 cal yr B.P. The area was influenced by extensive sea ice cover and iceberg transport with low foraminiferal fluxes and low primary production. The resulting summer $sSST_{Transfer}$ ranged from 1.9 to 2.7°C with an average of 2.1°C. However, the quantitative reconstructions based on Mg/Ca ratios show water temperatures ranging from 1.9 to 5.2°C with an average of 3.5°C during this time interval pointing to warmer conditions in those water masses where *N. pachyderma* calcified its test. This could possibly be ascribed to subsurface advection of Atlantic Water masses combined with shifts in the calcification season and/or the habitat depth of the foraminifera.

After ca. 10,300 cal yr B.P. ocean surface conditions ameliorated as *Turborotalita quinqueloba* rapidly became the dominating species and Atlantic Water inflow intensified, resulting in increased summer $sSST_{Transfer}$ ranging from 3.3 to 6.5°C (average 5.5°C). Moreover the flux of planktic foraminifera increased and influence from sea ice and icebergs diminished as the Arctic Front retreated north-westward. Concurrently the $sSST_{Mg/Ca}$ recorded by *N. pachyderma* showed values between 2.5 to 5.5°C with an average of 4.0°C which is an increase in average $sSST_{Mg/Ca}$ of only ~0.5°C compared to the preceding period. The relatively modest increase of $sSST_{Mg/Ca}$ compared to $sSST_{Transfer}$ was probably caused by a deepening of the habitat depth and/or a shift in the main calcification season for *N. pachyderma* during this period.

Acknowledgements

This work has been carried out within the framework of the International Polar Year project "Arctic Natural Climate and Environmental Changes and Human Adaption: From Science to Public Awareness" (SciencePub, IPY # 39) funded by the Research Council of Norway and the Trainee School in Arctic Marine Geology and

Geophysics, University of Tromsø. K.W. and R.F.S. received funding from the German Science Foundation (DFG) Priority Core Program 1266 INTERDYNAMIK (project HOVAG). Further the NFR project "*Changes in flux of Atlantic Water from the Nordic Seas to the Arctic Ocean during the late glacial and the Holocene"* partly funded the research. Sediment core and CTD data were collected onboard the R/V "Maria S. Merian" during the MSM05/5b expedition led by G. Budeus, Alfred Wegener Institute for Polar and Marine Research, Germany. J. P. Holm prepared the area map. Samples were prepared at the laboratory at Department of Geology, University of Tromsø by T. Dahl. K. Pascher and L. Haxhiaj assisted in foraminifer selection and stable isotope analyses at GEOMAR Helmholtz Centre for Ocean Research Kiel. Lennart de Nooijer and an anonymous person reviewed the manuscript. To these persons and institutions we offer our sincere thanks.

References

Aagaard, K., Foldvik, A., Hillman, S.R., 1987. The West Spitsbergen Current: disposition and water mass transformation. Journal of Geophysical Research, 92, 3778–3784.

623 Aagaard, K., Carmack, E.C., 1989. The role of sea ice and other fresh water in the Arctic circulation. Journal of
624 Geophysical Research, 94(C14), 14485-14498.

625 Aagaard-Sørensen, S., Husum, K., Hald, M., Marchitto, T., and Godtliebsen, F., 2013, Sub sea surface
626 temperatures in the Polar North Atlantic during the Holocene: Planktic foraminiferal Mg/Ca
627 temperature reconstructions. The Holocene, 24, 93-103.

628 Barker, S., Greaves, M., Elderfield, H., 2003. A study of cleaning procedures used for foraminiferal Mg/Ca
629 paleothermometry. Geochemistry, Geophysics, Geosystems, 4, doi: 10.1029/2003gc000559

630 Barker, S., Cacho, I., Benway, H., Tachikawa, K., 2005. Planktonic foraminiferal Mg/Ca as a proxy for past
631 oceanic temperatures: a methodological overview and data compilation for the Last Glacial Maximum.
632 Quaternary Science Reviews, 24, 821-834.

633 Birgel, D., Hass, H.C., 2004. Oceanic and atmospheric variations during the last deglaciation in the
634 Fram Strait (Arctic Ocean): a coupled high-resolution organic-geochemical and
635 sedimentological study. Quaternary Science Reviews, 23(1-2), 29-47.

636 Birks, H.J.B., 1995. Quantitative palaeoenvironmental reconstructions. In: Maddy, D., Brew, J.S. (Eds.),
637 Statistical Modelling of Quaternary Science Data. Quaternary Research Association, Cambridge, UK,
638 pp. 116–254.

639 Björck, S., Rundgren, M., Ingólfsson, Ó., Funder, S., 1997. The Preboreal oscillation around the Nordic Seas:
640 terrestrial and lacustrine responses. Journal of Quaternary Science, 12(6), 455-465.

641 Blindheim, J., Rey, F., 2004. Water-mass formation and distribution in the Nordic Seas during the 1990s. ICES
642 Journal of Marine Science, 61(5), 846-863.

643 Boltovskoy, E., Boltovskoy, D., Correa, N., Brandini, F., 1996. Planktic foraminifera from the southwestern
644 Atlantic (30°–60°S): species-specific patterns in the upper 50 m. Marine Micropaleontology, 28, 53-72.

645 Boyle, E.A., Keigwin, L.D., 1985. Comparison of Atlantic and Pacific paleochemical records for the last
646 215,000 years: changes in deep ocean circulation and chemical inventories. Earth and Planetary
647 Science Letters 76, 135-150.

Boyle, E.A., Rosenthal, Y., 1996. Chemical hydrography of the South Atlantic during the Last Glacial Maximum: Cd and d13C, in The South Atlantic: Present and Past Circulation. Edited by G. Wefer et al. Springer-Verlag, New York, 423-443.

Bourke, R.H., Weigel, A.M., Paquette, R.G., 1988. The Westward Turning Branch of the West Spitsbergen Current. Journal of Geophysical Research, 93, 14065-14077.

Bradley, R.S., England, J.H., 2008. The Younger Dryas and the Sea of Ancient Ice. Quaternary Research, 70**,** 1-10.

Broecker, W.S., Kennett, J.P., Flower, B.P., Teller, J.T., Trumbore, S., Bonani, G., Wolfli, W., 1989. Routing of meltwater from the Laurentide Ice Sheet during the Younger Dryas cold episode. Nature 341. 318–321

Carstens, J., Hebbeln, D., Wefer, G., 1997. Distribution of planktic foraminifera at the ice margin in the Arctic (Fram Strait). Marine Micropaleontology, 29(3-4), 257-269.

Conan, S.M.H., Ivanova, E.M., Brummer, G.J.A., 2002. Quantifying carbonate dissolution and calibration of foraminiferal dissolution indices in the Somali Basin. Marine Geology, 182**,** 325-349.

Darling, K.F., Kucera, M., Kroon, D., Wade, C.M., 2006. A resolution for the coiling direction paradox in Neogloboquadrina pachyderma. Paleoceanography, 21(2): PA2011, doi: 10.1029/2005pa001189

Ebbesen, H., Hald, M., Eplet, T.H., 2007. Late glacial and early Holocene climatic oscillations on the western Svalbard margin, European Arctic. Quaternary Science Reviews, 26(15-16): 1999-2011.

Elderfield, H., Ganssen, G.M., 2000. Past temperature and $d^{18}O$ of surface ocean waters inferred from foraminiferal Mg/Ca ratios. Nature, 405, 442–445.

Elderfield, H., Vautravers, M., Cooper, M., 2002. The relationship between shell size and Mg/Ca, Sr/Ca, $\delta^{18}O$, and $\delta^{13}C$ of species of planktonic foraminifera. Geochemistry, Geophysics, Geosystems, 3(8). doi:10.1029/2001gc000194.

Fairbanks, R.G., 1989. A 17,000-year glacio-eustatic sea level record: influence of glacial melting rates on the Younger Dryas event and deep-ocean circulation. Nature (London), 342, 637-642.

672 Farmer, E.J., Chapman, M.R., Andrews, J.E., 2008. Centennial-scale Holocene North Atlantic surface
673 temperatures from Mg/Ca ratios in *Globigerina bulloides*. Geochemistry, Geophysics, Geosystems, 9.
674 doi:10.1029/2008GC002199.

675 Hald, M., Aspeli, R., 1997. Rapid climatic shifts of the nothern Norwegian Sea during the last deglaciation and
676 the Holocene. Boreas, 26, 15-28.

677 Hald, M., Hagen, S., 1998. Early preboreal cooling in the Nordic Sea region triggered by meltwater. Geology
678 26, 615-618.

679 Hald, M., Andersson, C., Ebbesen, H., Jansen, E., Klitgaard-Kristensen, D., Risebrobakken, B., Salomonsen, G.
680 R., Sejrup, H. P., Sarnthein, M., Telford, R., 2007. Variations in temperature and extent of Atlantic
681 Water in the northern North Atlantic during the Holocene. Quaternary Science Reviews, 26, 3423-
682 3440.

683 Hop, H., Falk-Petersen, S., Svendsen, H., Kwasniewski, S., Pavlov, V., Pavlova, O., and Søreide, J.E., 2006,
684 Physical and biological characteristics of the pelagic system across Fram Strait to Kongsfjorden.
685 Progress In Oceanography, 71, 182-231.

686 Hopkins, T.S., 1991, The GIN Sea-A synthesis of its physical oceanography and literature review 1972-1985.
687 Earth-Science Reviews, 30, 175-318.

688 Hughen, K.A., Baillie, M.G.L., Bard, E., Beck, J.W., Bertrand, C.J.H., Blackwell, P.G., Buck, C.E., Burr, G.S.,
689 Cutler, K.B., Damon, P.E., Edwards, R.L., Fairbanks, R.G., Friedrich, M., Guilderson, T.P., Kromer,
690 B., McCormac, G., Manning, S., Ramsey, C.B., Reimer, P.J., Reimer, R.W., Remmele, S., Southon,
691 J.R., Stuiver, M., Talamo, S., Taylor, F.W., van der Plicht, J., Weyhenmeyer, C.E., 2004. Marine04
692 marine radiocarbon age calibration, 0-26 cal kyr BP. Radiocarbon 46, 1059-1086.

693 Husum, K., Hald, M., 2002. Early Holocene cooling events in Malangenfjord and the adjoining shelf, north-east
694 Norwegian Sea. Polar Research, 21(2), 267-274.

695 Husum, K., Hald, M., 2004. Modern Foraminiferal Distribution in the Subarctic Malangen Fjord and adjoining
696 Shelf, Northern Norway. Journal of Foraminiferal Research, 34(1), 34-48.

Husum, K., Hald, M. 2012. Arctic planktic foraminiferal assemblages: Implications for subsurface temperature reconstructions, Marine Micropaleontology 96–97(0), 38-47.

IPCC., 2007. Climate Change 2007: The physical science basis. Summary for policymakers, intergovernmental panel on climate change. Fourth Assessment Report, Geneva, IPCC Secretariat, 1–18.

Jennings, A.E., Hald, M., Smith, M., Andrews, J.T., 2006. Freshwater forcing from the Greenland Ice Sheet during the Younger Dryas: evidence from southeastern Greenland shelf cores. Quaternary Science Reviews, 25(3-4), 282-298.

Jessen, S.P., Rasmussen, T.L., Nielsen, T., Solheim, A., 2010. A new Late Weichselian and Holocene marine chronology for the western Svalbard slope 30,000-0 cal years BP. Quaternary Science Reviews, 29(9-10), 1301-1312.

Johannessen, T., Jansen, E., Flatøy, A., Ravalo, A.C., 1994. The relationship between surface water masses, oceanographic fronts and paleoclimatic proxies in surface sediments of the Greenland, Iceland and Norwegian Seas. NATO ASI series I, 17, 61-85.

Jonkers, L., Brummer, G.-J.A., Peeters, F.J.C., van Aken, H. M., De Jong, M.F., 2010. Seasonal stratification, shell flux, and oxygen isotope dynamics of left-coiling *N. pachyderma* and *T. quinqueloba* in the western subpolar North Atlantic. Paleoceanography 25, PA2204. Doi: 10.1029/2009pa001849

Juggins, S., 2010. C2, Version 1.6. 6. Software for Ecological and Palaeoecological Data Analysis and Visualization. University of Newcastle, Newcastle upon Tyne, UK. http://www.campus.ncl.ac.uk/staff/Stephen.Juggins/index.html.

Katz, M.E., Cramer, B.S., Franzese, A., Honisch, B., Miller, K.G., Rosenthal, Y., Wright, J.D., 2010. Traditional and emerging geochemical proxies in foraminifera. Journal of Foraminiferal Research, 40**,** 165-192.

Kaufman, D.S., Ager, T.A., Anderson, N.J., Anderson, P.M., Andrews, J.T., Bartlein, P.J., Brubaker, L.B., Coats, L.L., Cwynar, L.C., Duvall, M.L., Dyke, A.S., Edwards, M.E., Eisner, W.R., Gajewski, K., Geirsdottir, A., Hu, F.S., Jennings, A.E., Kaplan, M.R., Kerwin, M.W., Lozhkin, A.V., MacDonald, G.M., Miller, G.H., Mock, C.J., Oswald, W.W., Otto-Bliesner, B.L., Porinchu, D.F., Ruhland, K.,

Smol, J.P., Steig, E.J., Wolfe, B.B., 2004. Holocene thermal maximum in the western Arctic (0-180°W). Quaternary Science Reviews, 23, 529-560.

Knies, J., Hald, M., Ebbesen, H., Mann, U., Vogt, C., 2003. A deglacial—middle Holocene record of biogenic sedimentation and paleoproductivity changes from the northern Norwegian continental shelf. Paleoceanography, 18(4): 1096, doi:10.1029/2002PA000872,.

Koç, N., Jansen, E., Haflidason, H., 1993. Paleoceanographic reconstructions of surface ocean conditions in the Greenland, Iceland and Norwegian seas through the last 14 ka based on diatoms. Quaternary Science Reviews, 12(2), 115-140.

Koç, N., Klitgaard-Kristensen, D., Hasle, K., Forsberg, C.F., Solheim, A., 2002. Late glacial palaeoceanography of Hinlopen Strait, northern Svalbard. Polar Research, 21(2), 307-314.

Kozdon, R., Eisenhauer, A., Weinelt, M., Meland, M.Y., Nürnberg, D., 2009. Reassessing Mg/Ca temperature calibrations of *Neogloboquadrina pachyderma* (sinistral) using paired δ44/40Ca and Mg/Ca measurements. Geochemistry, Geophysics, Geosystems, 10. Doi:10.1029/2008GC002169

Kucera, M., Weinelt, M., Kiefer, T., Pflaumann, U., Hayes, A., Weinelt, M., Chen, M.-T., Mix, A.C., Barrows, T.T., Cortijo, E., Duprat, J., Juggins, S., Waelbroeck, C., 2005. Reconstruction of sea-surface temperatures from assemblages of planktonic foraminifera: multi-technique approach based on geographically constrained calibration data sets and its application to glacial Atlantic and Pacific Oceans. Quaternary Science Reviews, *24*(7-9), 951-998.

Landvik, J.Y., Bondevik, S., Elverhoi, A., Fjeldskaar, W., Mangerud, J., Salvigsen, O., Siegert, M.J., Svendsen, J.-I., Vorren, T. O., 1998. The last glacial maximum of Svalbard and the Barents sea area: ice sheet extent and configuration. Quaternary Science Reviews, 17(1-3), 43-75.

Le, J., Shackleton, N.J., 1992. Carbonate Dissolution Fluctuations in the Western Equatorial Pacific During the Late Quaternary. Paleoceanography, 7(1), 21-42.

Lea, D.W., Mashiotta, T.A., Spero, H.J., 1999. Controls on magnesium and strontium uptake in planktonic foraminifera determined by live culturing. Geochimica et Cosmochimica Acta, 63, 2369-2379.

748 Loeng, H., Ozhigin, V., Ådlandsvik, B., 1997. Water fluxes through the Barents Sea. ICES Journal of Marine
749 Science, 54(3), 310-317.

750 Lombard, F., Labeyrie, L., Michel, E., Spero, H.J., Lea, D.W., 2009. Modelling the temperature dependent
751 growth rates of planktic foraminifera. Marine Micropaleontology, 70(1-2), 1-7.

752 Mangerud, J., Gulliksen, S., 1975. Apparent radiocarbon ages of Recent marine shells from Norway,
753 Spitsbergen, and Arctic Canada. Quaternary Research, 5, 263-273.

754 Mangerud, J., Bondevik, S., Gulliksen, S., Hufthammer, A.K., Høisæter, T. 2006. Marine14 C reservoir ages for
755 19th century whales and molluscs from the North Atlantic. Quaternary Science Reviews, 25, 3228-
756 3245.

757 Manley, T.O., 1995. Branching of Atlantic Water within the Greenland-Spitsbergen passage: An estimate of
758 recirculation. Journal of Geophysical Research, 100, 20627-20634.

759 Marchitto, T.M., 2006. Precise multielemental ratios in small foraminiferal samples determined by sector field
760 ICP-MS. Geochemistry, Geophysics, Geosystems, 7. Doi: 10.1029/2005gc001018

761 Marnela, M., Rudels, B., Olsson, K.A., Anderson, L.G., Jeansson, E., Torres, D.J., Messias, M.-J., Swift, J.H.,
762 Watson, A. J., 2008. Transports of Nordic Seas water masses and excess SF6 through Fram Strait to the
763 Arctic Ocean, Progress In Oceanography, 78(1), 1-11.

764 Nürnberg, D., Bijma, J., Hemleben, C., 1996. Assessing the reliability of magnesium in foraminiferal
765 calcite as a proxy for water mass temperatures. Geochimica et Cosmochimica Acta, 60(5),
766 803-814.

767 Pados, T., Spielhagen, R.F., in press. Species distribution and depth habitat of recent planktic foraminifera in the
768 Fram Strait (Arctic Ocean). Polar Research

769 Peltier, W.R., and Fairbanks, R.G., 2006. Global glacial ice volume and Last Glacial Maximum duration from
770 an extended Barbados sea level record. Quaternary Science Reviews, 25, 3322-3337.

771 Pfuhl, H.A., Shackleton, N.J., 2004. Two proximal, high-resolution records of foraminiferal fragmentation and
772 their implications for changes in dissolution. Deep Sea Research Part I: Oceanographic Research
773 Papers, 51(6), 809-832.

774 Rasmussen, S.O., Andersen, K.K., Svensson, A.M., Steffensen, J.P., Vinther, B.M., Clausen, H.B., Siggaard-
775 Andersen, M.-L., Johnsen, S.J., Larsen, L.B., Dahl-Jensen, D., Bigler, R., Röthlisberger, M., Fischer,
776 H., Goto-Azuma, K., Hansson, M.E., and Ruth, U., 2006. A new Greenland ice core chronology for the
777 last glacial termination. Journal of Geophysical Research, 111, 16 pp, doi:10.1029/2005JD006079.

778 Rasmussen, S.O., Vinther, B.M., Clausen, H.B., Andersen, K.K., 2007a. Early Holocene climate oscillations
779 recorded in three Greenland ice cores. Quaternary Science Reviews, 26, 1907-1914.

780 Rasmussen, T.L., Thomsen, E., Ślubowska, M.A., Jessen, S., Solheim, A., Koç, N., 2007b. Paleoceanographic
781 evolution of the SW Svalbard margin (76^0N) since 20,000 ^{14}C yr BP. Quaternary Research, 67(1), 100-
782 114.

783 Reimer, P.J., Baillie, M.G.L., Bard, E., Bayliss, A., Beck, J.W., Bertrand, C.J.H., Blackwell, P.G., Buck, C.E.,
784 Burr, G.S., Cutler, K.B., Damon, P.E., Edwards, R. L., Fairbanks, R.G., Friedrich, M., Guilderson,
785 T.P., Hogg, A.G., Hughen, K.A., Kromer, B., McCormac, F.G., Manning, S.W., Ramsey, C.B.,
786 Reimer, R.W., Remmele, S., Southon, J.R., Stuiver, M., Talamo, S., Taylor, F.W., van der Plicht, J.,
787 Weyhenmeyer, C.E., 2004. IntCal04 Terrestrial radiocarbon age calibration, 26 - 0 ka BP. Radiocarbon
788 46, 1029-1058.

789 Reimer, P.J., Baillie, M.G.L., Bard, E., Bayliss, A., Beck, J.W., Blackwell, P.G., Bronk Ramsey, C., Buck, C.E.,
790 Burr, G.S., Edwards, R.L., Friedrich, M., Grootes, P.M., Guilderson, T.P., Hajdas, I., Heaton, T.J.,
791 Hogg, A.G., Hughen, K.A., Kaiser, K.F., Kromer, B., McCormac, F.G., Manning, S.W., Reimer, R.W.,
792 Richards, D.A., Southon, J.R., Talamo, S., Turney, C.S.M., van der Plicht, J., Weyhenmeyer, C.E.,
793 2009. IntCal09 and Marine09 Radiocarbon Age Calibration Curves, 0–50,000 Years cal BP.
794 Radiocarbon 51, 1111–1150.

795 Risebrobakken, B., Dokken, T., Smedsrud, L.H., Andersson, C., Jansen, E., Moros, M., Ivanova, E.V., 2011.
796 Early Holocene temperature variability in the Nordic Seas: The role of oceanic heat advection versus
797 changes in orbital forcing. Paleoceanography, 26, PA4206.

798 Rudels, B., Friedrich, H.J., Quadfasel, D., 1999. The Arctic Circumpolar Boundary Current. Deep Sea Research
799 Part II: Topical Studies in Oceanography, 46, 1023-1062.

800 Rudels, B., Björk, G., Nilsson, J., Winsor, P., Lake, I., Nohr, C., 2005. The interaction between waters from the
801 Arctic Ocean and the Nordic Seas north of Fram Strait and along the East Greenland Current: results
802 from the Arctic Ocean-02 Oden expedition, Journal of Marine Systems, 55(1-2), 1-30.

803 Sarnthein, M., Jansen, E., Weinelt, M., Arnold, M., Duplessy, J. C., Erlenkeuser, H., Flatøy, A., Johannessen,
804 G., Johannessen, T., Jung, S., Koc, N., Labeyrie, L., Maslin, M., Pflaumann, U., Schulz, H., 1995.
805 Variations in Atlantic surface ocean paleoceanography, 50°-80°N: A time-slice record of the last
806 30,000 years. Paleoceanography, 10(6), 1063–1094.

807 Sarnthein, M., Van Kreveld, S., Erlenkeuser, H., Grootes, P.M., Kucera, M., Pflaumann, U., Schulz, M., 2003.
808 Centennial-to-millennial-scale periodicities of Holocene climate and sediment injections off the
809 western Barents shelf, 75°N. Boreas, 32, 447- 461.

810 Schauer, U., Loeng, H., Rudels, B., Ozhigin, V.K., Dieck, W., 2002. Atlantic Water flow through the Barents
811 and Kara Seas. Deep Sea Research Part I: Oceanographic Research Papers, 49(12), 2281-2298.

812 Schauer, U., Fahrbach, E., Osterhus, S., Rohardt, G., 2004. Arctic warming through the Fram Strait: Oceanic
813 heat transport from 3 years of measurements. Journal of Geophysical Research, 109: C06026,
814 doi:10.1029/2003JC001823.

815 Schauer, U., Beszczynska-Möller, A., 2009. Problems with estimation and interpretation of oceanic heat
816 transport - conceptual remarks for the case of Fram Strait in the Arctic Ocean. Ocean Science, 5(4),
817 487-494.

818 Simstich, J., Sarnthein, M., Erlenkeuser, H., 2003. Paired delta O-18 signals of *Neogloboquadrina pachyderma*
819 (s) and *Turborotalita quinqueloba* show thermal stratification structure in Nordic Seas. Marine
820 Micropaleontology, 48, 107-125.

821 Skirbekk, K., Kristensen, D.K., Rasmussen, T.L., Koç, N., Forwick, M., 2010. Holocene climate variations at
822 the entrance to a warm Arctic fjord: evidence from Kongsfjorden trough, Svalbard. Geological Society,
823 London, Special Publications, 344, 289-304.

824 Ślubowska, M., Koç, N., Rasmussen, T.L., Klitgaard-Kristensen, D., 2005. Changes in the flow of Atlantic
825 water into the Arctic Ocean since the last deglaciation: Evidence from the northern Svalbard
826 continental margin, 80°N. Paleoceanography, 20: PA001141.

827 Ślubowska-Woldengen, M., Rasmussen, T.L., Koç, N., Klitgaard-Kristensen, D., Nilsen, F., Solheim, A., 2007.
828 Advection of Atlantic Water to the western and northern Svalbard shelf since 17,500 cal yr BP.
829 Quaternary Science Reviews, 26(3-4), 463-478.

830 Ślubowska-Woldengen, M., Koç, N., Rasmussen, T.L., Klitgaard-Kristensen, D., Hald, M., Jennings, A.E.,
831 2008. Time-slice reconstructions of ocean circulation changes on the continental shelf in the Nordic
832 and Barents Seas during the last 16,000 cal yr B.P. Quaternary Science Reviews, 27(15-16), 1476-
833 1492.

834 Spielhagen, R.F., Erlenkeuser, H., 1994. Stable oxygen and carbon isotopes in planktic foraminifers from Arctic
835 Ocean surface sediments: Reflection of the low salinity surface water layer. Marine Geology, 119**,** 227-
836 250.

837 Spielhagen, R.F., Werner, K., Sørensen, S.A., Zamelczyk, K., Kandiano, E., Budeus, G., Husum, K., Marchitto,
838 T.M., Hald, M., 2011. Enhanced Modern Heat Transfer to the Arctic by Warm Atlantic Water. Science,
839 331**,** 450-453.
840
841 Steffensen, J.P., Andersen, K.K., Bigler, M., Clausen, H.B., Dahl-Jensen, D., Fischer, H., Goto-Azuma, K.,
842 Hansson, M., Johnsen, S.J., Jouzel, J., Masson-Delmotte, V., Popp, T., Rasmussen, S.O., Rothlisberger,
843 R., Ruth, U., Stauffer, B., Siggaard-Andersen, M.-L., Sveinbjornsdottir, A.E., Svensson, A., White,
844 J.W.C. 2008. High-Resolution Greenland Ice Core Data Show Abrupt Climate Change Happens in Few
845 Years. Science, 321, 680-684.

846 Stuiver, M., Reimer, P.J., Reimer, R.W., 2005. CALIB 6.0. [WWW program and documentation].

847 Swift, J.H., and Aagaard, K., 1981, Seasonal transitions and water mass formation in the Iceland and Greenland
848 seas: Deep Sea Research Part A. Oceanographic Research Papers, 28, 1107-1129.

Ter Braak, C.J.F., Juggins, S., 1993. Weighted averaging partial least-squares regression (WA-PLS) - an improved method for reconstructing environmental variables from species assemblages. Hydrobiologia, 269, 485–502.

Volkmann, R., 2000. Planktic foreminifers in the outer Laptev Sea and the Fram Strait - Modern distribution and ecology. Journal of Foraminiferal Research, 30(3), 157-176.

Walczowski, W., Piechura, J., Osinski, R., Wieczorek, P., 2005. The West Spitsbergen Current volume and heat transport from synoptic observations in summer. Deep Sea Research Part I: Oceanographic Research Papers, 52(8), 1374-1391.

Walker, M., Johnsen, S., Rasmussen, S.O., Popp, T., Steffensen, J.-P., Gibbard, P., Hoek, W., Lowe, J., Andrews, J., Björck, S., Cwynar, L.C., Hughen, K., Kershaw, P., Kromer, B., Litt, T., Lowe, D.J., Nakagawa, T., Newnham, R., Schwander, J., 2009. Formal definition and dating of the GSSP (Global Stratotype Section and Point) for the base of the Holocene using the Greenland NGRIP ice core, and selected auxiliary records. Journal of Quaternary Science, 24, 3-17.

Werner, K, Spielhagen, R.F., Bauch D., Hass, H.C., Kandiano, E., 2013. Atlantic Water advection versus sea-ice advances in the eastern Fram Strait during the last 9 ka – multiproxy evidence for a two-phase Holocene. Paleoceanography, 28(2), 283-295.

Wollenburg, J.E., Knies, J., Mackensen, A., 2004. High-resolution paleoproductivity fluctuations during the past 24 kyr as indicated by benthic foraminifera in the marginal Arctic Ocean. Palaeogeography, Palaeoclimatology, Palaeoecology, 204, 209-238.

Woodgate, R.A., Fahrbach, E., Rohardt, G., 1999. Structure and transports of the East Greenland Current at 75°N from moored current meters. Journal of Geophysical Research, 104(C8): 18059-18072.

Zamelczyk, K., Rasmussen, T.L., Husum, K., Haflidason, H., de Vernal, A., Ravna, E.K., Hald, M., Hillaire-Marcel, C., 2012. Paleoceanographic changes and calcium carbonate dissolution in the central Fram Strait during the last 20 ka yr. Quaternary Research, doi.10.1016/j.yqres.2012.07.006

874 **Figure captions**

875 **Table 1.** Radiocarbon dates and calibrations from core MSM5/5-712-2.

876 **Table 2.** Performance of transfer function model WA-PLS with components 1 to 5. Selected
877 model indicated in bold letters.

878 **Figure 1.** (A) Map of the north-eastern North Atlantic Ocean and adjoining seas showing the
879 major currents systems and average position of the Polar and Arctic fronts modified
880 from Marnela et al. (2008). Location of Kastenlot core MSM05/5-712-2 indicated by
881 a double circle and other cores (Hald and Aspeli, 1997 (T-88-2); Ebbesen et al., 2007
882 (MD99-2304)) by open circles. Abbreviations: NwASC: Norwegian Atlantic Slope
883 Current; NwAC: Norwegian Atlantic Current; WSC: West Spitsbergen Current;
884 NCaC: North Cape Current; RAW: Re-circulating Atlantic Water; SB: Svalbard
885 Branch; YSC: Yermark Slope Current; ESC: East Spitsbergen Current; EGC: East
886 Greenland Current. (B) Temperature and salinity profile from the core site measured
887 in August 2007.

888 **Figure 2.** Age model and sedimentation rate of core MSM05/5-712-2. Error bars show the 2σ
889 standard deviation of the calibrated ages.

890 **Figure 3.** Planktic foraminifera, sedimentological and geochemical data plotted against age
891 and depth in core MSM05/5-712-2. (A) Bulk sediment calcium carbonate ($CaCO_3$)
892 (wt.%) (Aagaard-Sørensen et al., 2013 and present study); (B) Total flux of planktic
893 foraminifera on logarithmic scale (grey shading); (C-G) Relative percentage of five
894 most abundant planktic foraminiferal species (black lines); (H-L) Flux of individual
895 species (grey shading); (M) Grain size >1mm (IRD); (N) Selected grain sizes (weight
896 %) >63µm and <63µm and lithological units; (O) Diatom-rich layer (vertical light

grey shading). Chronostratigraphical zones follow Rasmussen et al. (2007a), Steffensen et al. (2008) and Walker et al. (2009). Diamonds on X-axis indicate radiocarbon dated levels.

Figure 4. Planktic foraminiferal stable isotopes, trace elements and fragmentation plotted against age and depth in core MSM05/5-712-2. (A) % fragmentation; (B) $\delta^{13}C$ in *N. pachyderma*. Error bar shows analytical precision (±0.03‰); (C) Ice-volume corrected and uncorrected $\delta^{18}O$ (black line: Fairbanks, 1989; grey line: Peltier and Fairbanks, 2006; thin grey line: uncorrected data) in *N. pachyderma*. Error bar shows analytical precision (±0.06‰); (D) Mg/Ca in *N. pachyderma* (Aagaard-Sørensen et al., 2013 and present study). The thin line shows the raw data, and the thick line is the five-point running mean. The crosses mark omitted data points. The filled circle shows the average reproducibility of sample splits (±0.049 mmol/mol); (E) Post cleaning mass of $CaCO_3$ (µg). Chronostratigraphical zones follow Rasmussen et al. (2007a), Steffensen et al. (2008) and Walker et al. (2009). Diamonds on X-axis indicate radiocarbon dated levels.

Figure 5. Foraminiferal records and sSST reconstruction from core MSM05/5-712-2 compared to other records from the Nordic Seas and the NorthGRIP ice core plotted against age. (A) Stable oxygen isotope ($\delta^{18}O$) record obtained from the NGRIP ice core (Rasmussen et al., 2006). (B) Reconstructed $sSST_{Mg/Ca}$ (black line) and $sSST_{Mg/Ca+15\%}$ based on Mg/Ca values that have been artificially increased 15 % (thin grey line) using the temperature equation of Kozdon et al. (2009). The $sSST_{Transfer}$ for 100 m water depth (Husum and Hald, 2012) (thick grey line). Triangles on Y-axis indicate modern water temperature at 25 (6.7°C) and 250 (3.7°C) m water depth in the Fram Strait (See Fig. 1B). (C) $sSST_{Transfer}$ reconstruction at 100 m water depth in core

MD99-2304 (thick grey line) (Ebbensen et al., 2007; Husum and Hald, 2012). (D) $sSST_{Transfer}$ reconstruction at 100 m water depth in core T-88-2 (thick grey line) (Hald and Aspeli, 1997; Husum and Hald, 2012). (E-G) Relative percentage of *T. quinqueloba* (grey shading) in core MSM05/5-712-2 (present study), MD99-2304 (Ebbesen et al., 2007) and T-88-2 (Hald and Aspeli, 1997). Chronostratigraphical zones follow Rasmussen et al. (2007a), Steffensen et al. (2008) and Walker et al. (2009).

Table 1

Lab. code	Depth range (cm)	Material	^{14}C age	Calibrated age ± 2σ	2 σ max cal. age (cal. age intercepts) 2 σ min cal. age	Reservoir age (R=400 + ΔR)	$\delta^{13}C$(‰)
Poz-30723	214-215	*N. pachyderma*	8362±45	cal. BP 8749 ±209	cal. BP 8540 (8749) 8958	551±51	-0.6 ± 0.4
KIA 37423	280-281	*N. pachyderma*	9220±50	cal. BP 9797±252	cal. BP 9551 (9797) 10042	551±51	-2.99 ± 0.35
Poz-30725	322-323	*N. pachyderma*	9580±47	cal. BP 10310 ±158	cal. BP 10152 (10310) 10468	551±51	-2.6 ± 0.1
Poz-30726	428-431	*N. pachyderma*	12358±63	cal. BP 13629±197	cal. BP 13432 (13629) 13826	551±51	-1.1 ± 0.1

Table 2

Model	RMSEP	r^2	Max Bias
WAPLS Component 1	0.56257	0.89493	0.63227
WAPLS Component 2	0.52205	0.90954	0.58702
WAPLS Component 3	**0.51659**	**0.91141**	**0.56346**
WAPLS Component 4	0.51718	0.91121	0.59419
WAPLS Component 5	0.52354	0.90902	0.59279

935 Fig 1

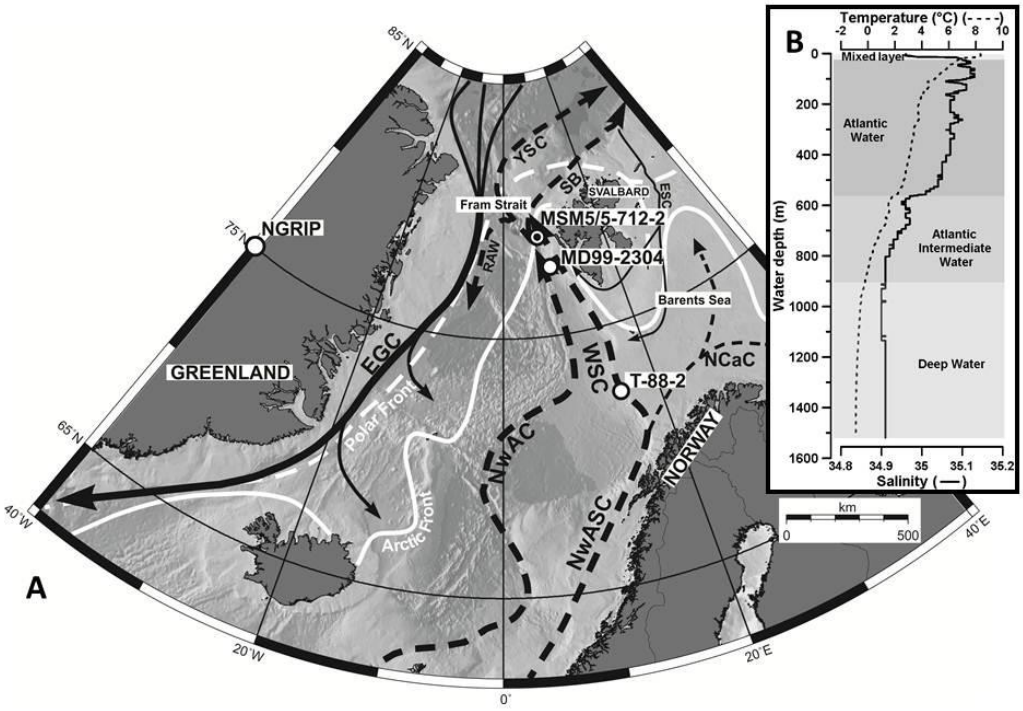

936

937 Fig 2

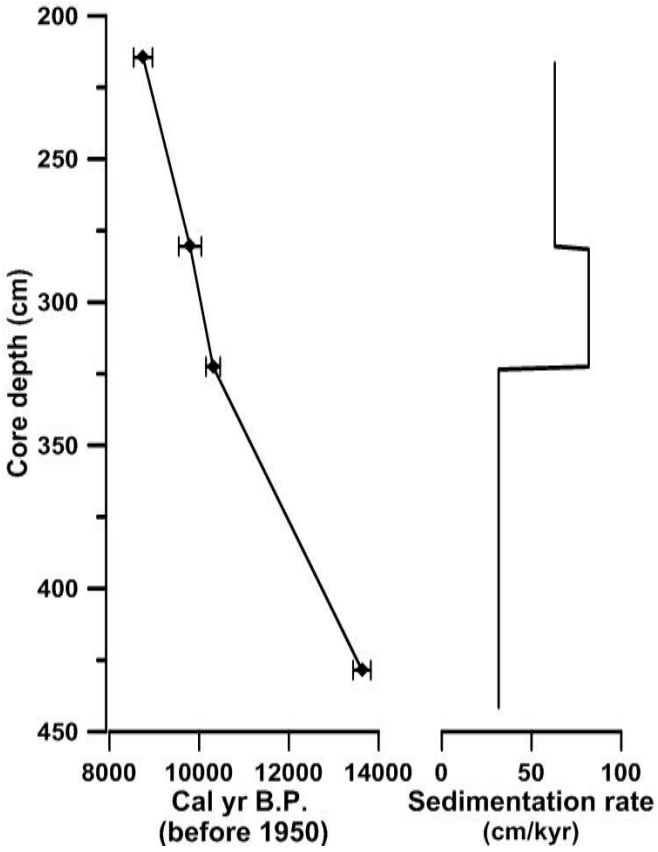

938

939 Fig 3

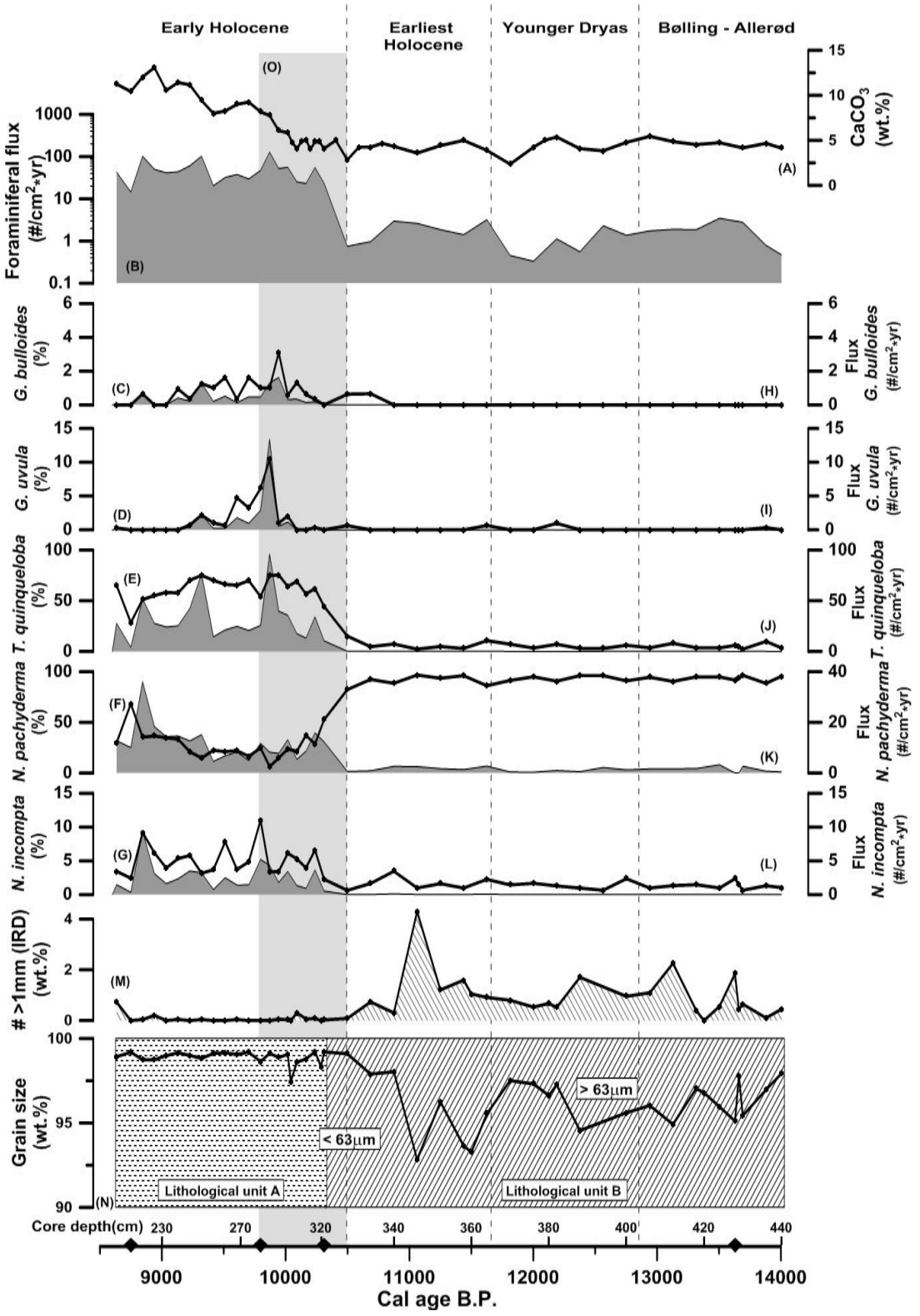

940

941

942

943 Fig 4

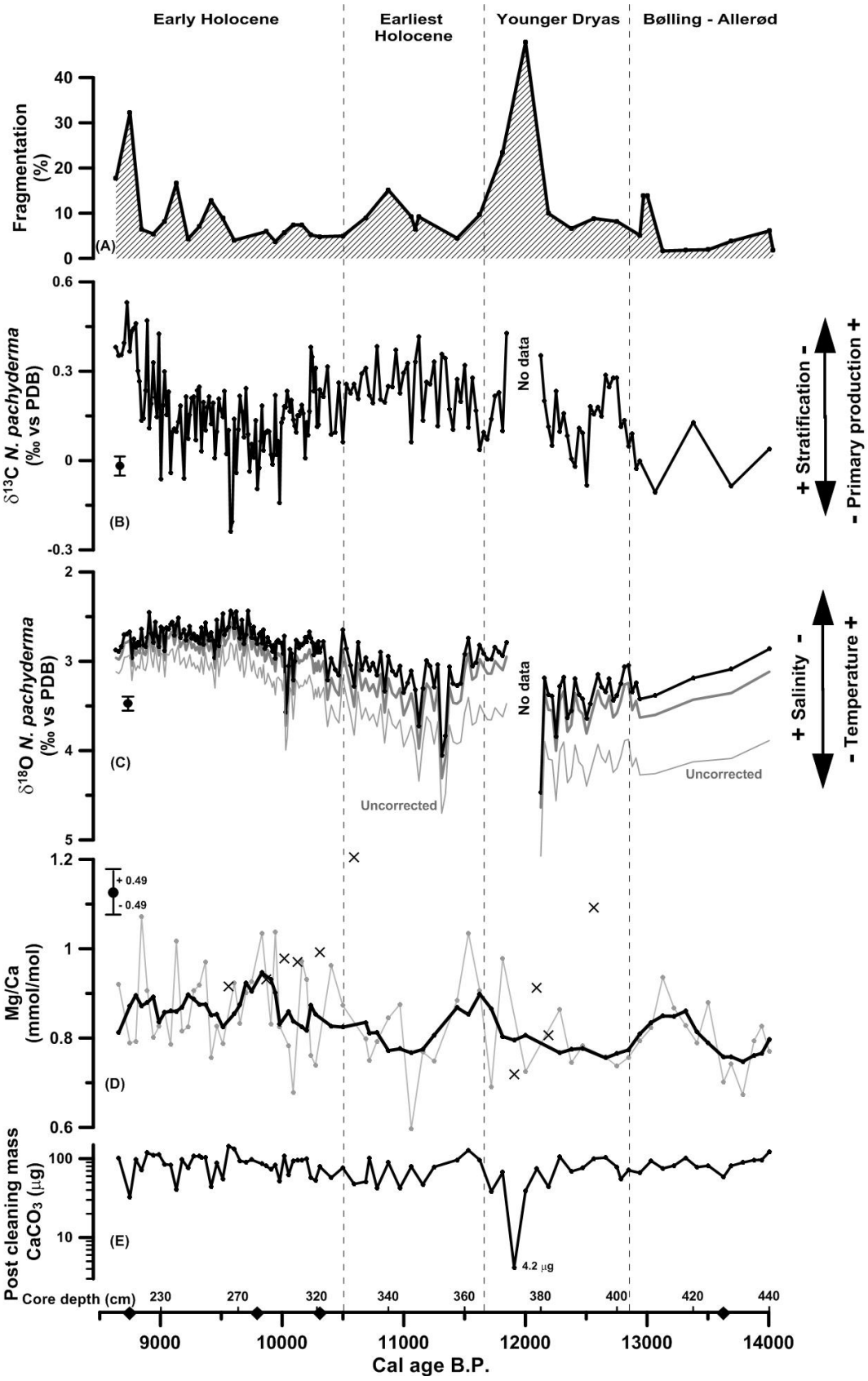
Early Holocene
Earliest Holocene
Younger Dryas
Bølling - Allerød
Fragmentation (%)
(A)
δ13C N. pachyderma (‰ vs PDB)
(B)
No data
+ Stratification -
- Primary production +
δ18O N. pachyderma (‰ vs PDB)
(C)
Uncorrected
No data
Uncorrected
+ Salinity -
- Temperature +
+ 0.49
- 0.49
Mg/Ca (mmol/mol)
(D)
Post cleaning mass CaCO3 (µg)
(E)
4.2 µg
Core depth (cm)
Cal age B.P.

944

945 Fig 5

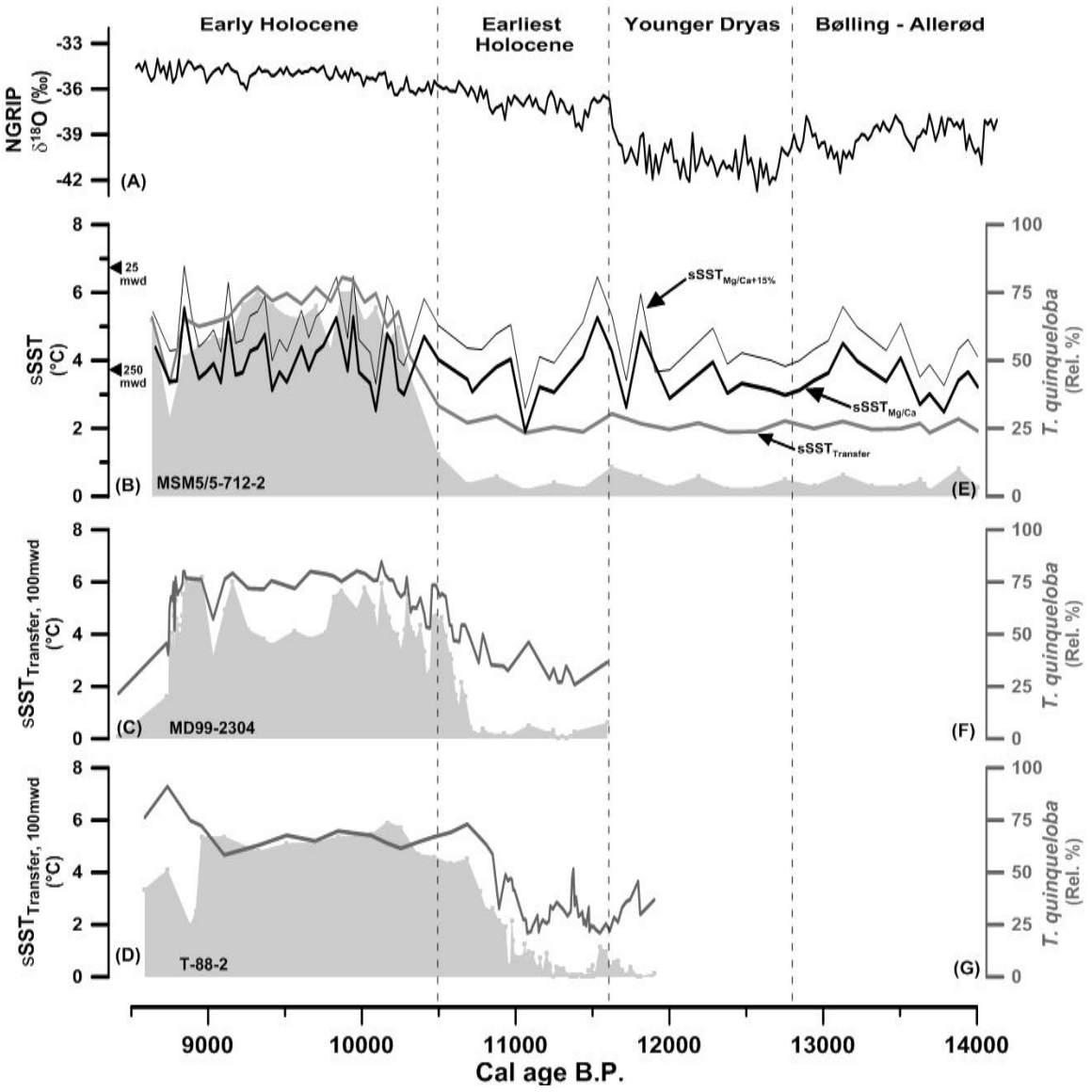
Early Holocene
Earliest Holocene
Younger Dryas
Bølling - Allerød
NGRIP δ18O (‰)
-33
-36
-39
-42
(A)
sSST (°C)
25 mwd
250 mwd
sSSTMg/Ca+15%
sSSTMg/Ca
sSSTTransfer
(B) MSM5/5-712-2
(E)
T. quinqueloba (Rel. %)
sSSTTransfer, 100mwd (°C)
(C) MD99-2304
(F)
(D) T-88-2
(G)
9000
10000
11000
12000
13000
14000
Cal age B.P.

946